CHAPTER IV
PREPARATION OF ELECTRICALLY CONDUCTIVE CELLULOSE BY AMMONIA GAS-ENHANCEING *IN SITU* SYNTHESIS OF SILVER PARTICLES INTO BACTERIAL CELLULOSE MATRIX

4.1 Abstract

In this study, the electrically conductive cellulose was successfully prepared by ammonia gas-enhancing *in situ* synthesis of silver nanoparticles into bacterial cellulose (BC) matrix. Briefly, BC pellicles were immersed in silver nitrate ($AgNO_3$) and glucose mixture solution. Then the precursors, silver ion (Ag^+) and glucose, absorbed-BC pellicle was treated with ammonia gas. By treating with ammonia gas, the Ag^+ was converted to Ag nanoparticle inside the nanofibrous matrix of BC. The synthetic route were modified the Tollens process by using the concept of the *in situ* synthesis in that the precursors, Ag^+ and glucose were firstly incorporated into the BC matrix. Then the precursor absorbed-BC was treated with ammonia gas. By using the ammonia gas-enhancing *in situ* synthesis process, silver nanoparticle were homogeneously dispersed in the matrix of BC. The effect of Ag^+ to glucose mole ratio on the particle size and particle size distribution of the as-prepared Ag nanoparticle was investigated by ultraviolet-visible spectroscopy (UV-Vis spectroscopy) and transmission electron microscope (TEM) with inbuilt energy dispersive X-ray analysis (EDX). By increasing the mole ratio of Ag^+: glucose from 10:1 to 100:1 and to 1000:1, the particle size of the as-prepared Ag particle was decrease from 27.19 ±8.63 to 17.27 ±6.25 and to 13.67 ±3.03 nm, respectively. The UV-Vis spectroscopy results were also corresponded to the particle size of the as-prepared Ag nanoparticle. The characteristic UV-Vis absorption peaks were shifted into the red shift and broaden with the large particle size and wide particle size distribution. The morphology of the as-prepared Ag nanoparticle-incorporated BC sample was investigated by Scanning Electron Microscope (SEM). The as-prepared Ag nanoparticles were clearly observed at the surface of nanofibril BC. The amount of Ag particles was increased and tended to aggregate with increasing the concentration of $AgNO_3$ in the precursor solution. The crystal structure of the Ag

investigated by X-ray diffraction (XRD) technique. The XRD patterns of the as-prepared Ag particle incorporated-BC samples which preparing by various preparation conditions were exhibited the similar XRD patterns with 4 characteristic diffraction peaks of Ag nanoparticle at $2\theta = 38.1°$, 44.3°, 64.4° and 78.0°. These evidences were clearly confirmed the successfully incorporating of silver nanoparticle into nanofibrous matrix of BC. The percent incorporation of Ag nanoparticle in the as-prepared Ag nanoparticle incorporated-BC samples were determined by thermogravimetric analysis (TGA). The percent incorporation of Ag nanoparticle in the as-prepared Ag nanoparticle incorporated-BC sample was increased with increasing the concentration of $AgNO_3$ in the precursor mixture solution. The percent incorporation of Ag nanoparticle in the as-prepared Ag nanoparticle incorporated-BC sample was increased from 9.80 ±0.53 to 25.09 ±0.46 and to 41.50 ±0.42 wt % with increasing of the $AgNO_3$ concentration from 0.01 to 0.025 and to 0.050 M, respectively. The percent incorporation of Ag nanoparticle was then reached to the saturation point with 49.17 ±0.51 wt % at the $AgNO_3$ concentration of 0.075 M. Finally, the electrical conductivity of the as-prepared Ag nanoparticle incorporated-BC samples was measured by using the two-point probe conductivity measurement. The electrical conductivity of the as-prepared Ag particle incorporated-BC samples were in the range between 10^{-4} S/cm to 10^{3} S/cm. The electrical conductivity of the as-prepared Ag nanoparticle incorporated-BC samples could be tailored made by adjusting the preparation condition. Therefore the as-prepared Ag particle incorporated-BC samples could also tailor made to be a semiconducting ($\sigma = 10^{-8}$–10^{3} S/cm) or conducting material ($\sigma > 10^{3}$ S/cm) by adjusting the preparation condition. All these evidences could be clearly revealed that the ammonia gas-enhancing *in situ* synthesis is one of the promising preparation methods for incorporating of Ag nanoparticle into the nanofibrous matrix of BC.

4.2 Introduction

Electrically responsive material is specific subsets of smart materials, in which conductive particles are dispersed in a polymer matrix, which can adaptively

change their physical properties due to an external electric field. Electrically responsive materials were expected to exhibit interesting electric field-dependent mechanical behavior with a wide range of potential applications such as electromagnetic interference shielding paper (Fugetsua, Sanob, Sunadac, Sambongic, Shibuyac, Wangd, & Hirakid, 2008), sensor (Thuwachaowsoan, Chotpattananont, Sirivat, Rujiravanit, & Schwank, 2007), actuator (Hiamtup, Sirivat, & Jamieson, 2008) and electrically stimuli control released hydrogel (Niamlang, & Sirivat, 2009). In general, electrically responsive materials were consisted of two main compositions which are conductive particles and polymer matrix.

Among the several kinds of conductive material such as gold, palladium, silver, nickel, copper, conductive polymer, graphite and carbon fiber, silver is one of the most interesting materials due to its excellent electrical, thermal, optical and/or catalytic properties (Lu, & Chou, 2008). Silver bulk exhibited the high electrical conductivity with 10^6 S/cm. Recently, nanometer-scaled silver have received a great deal of attention in various potential applications, such as conductors, catalysts, chemical sensors, etc. (Haes, & Van Duyne, 2003; Magdassi et al., 2003; Nie, & Emory, 1997; Pradhan, Pal, & Pal, 2002; Ye, Lai, Liu, & Tholen, 1999). Due to their small sizes and large surface-to-volume ratios, nanometer-scaled silver have superior properties compared to their bulk counterparts, they are promising candidates for novel nanoscale electronic, optical and mechanical devices. In order to achieve the high efficiency of electrical conduction, the most importance requirement is the connection of as-prepared nanometer-scaled silver; the particles need to be well connected to form the conduction pathway (Zhang, Moon, Lin, Agar, & Wong, 2011). However, the nanometer-scaled Ag still had limitations due to the extremely high surface area. The dispersion of the nanometer-scaled Ag in polymers or organic matrix was very difficult. It was always agglomerated to be a large particle with lacked of the desired-properties.

Acetobacter xylinum (*A. Xylinum*), a rod shaped aerobic gram negative bacterium which occurs as a contaminant in vinegar production. It produced a white gelatinous material (pellicle) on the surface of the liquid medium in a static culture system at 30–40°C (Dubey, Saxena, Singh, Ramana, & Chauhan 2002). That pellicle was a pure cellulose hydrogel and called "Bacterial cellulose (BC)". BC is produced

in the form of fibrous structure which constitutes to be a three-dimensional nonwoven network of nanofiber with diameters less than 100 nm. Basically, BC has the same chemical structure as plant cellulose, linear α-1,4-glucan chains (Czaja, Romanovicz, & Malcolm Brown, 2004) but the physical structure was completely different. The three-dimensional structure was only found in BC and not found in vascular plant cellulose (Rezaee, Solimani, & Forozandemogadam, 2005; Wan, Hong, Jia, Huang, Zhu, Wang, & Jiang, 2006; Grzegorczyn, & Ezak, 2007). This three-dimensional structure of BC resulted in high cellulose crystallinity (60–80%) and as high Young's modulus of 138 GPa and tensile strength of at least 2 GPa, which are almost equal to those of aramid fibers (Li, Chen, Hu, Shi, Shen, Zhang, & Wang, 2009). These unique properties of BC leading to wide range of applications such as paper industrial, headphone membranes, food industrial (Li, Chen, Hu, Shi, Shen, Zhang, & Wang, 2009), biomaterials including temporary skin substitute, artificial blood vessels (Czaja, Young, Kawecki, & Brown, 2007; Kamel, 2007) and membrane for pervaporation of water-ethanol binary mixtures (Dubey, Saxena, Singh, Ramana & Chauhan, 2002). In addition to these applications, there is also an important application for BC in terms of its unique three dimensional network structure of nanofiber. It serves as an applicable matrix for impregnating of nanoparticles or nanowires such as ZnO nanoparticles (Hu, Chen, Zhou, & Wang, 2010), CdS nanoparticles (Hu, Chen, Li, Shi, Shen, Zhang, & Wang, 2009), silver chloride nanoparticles (Hu, Chen, Li, Shi, Shen, Zhang, & Wang, 2009), silver nanoparticles (Maneerung, Tokura, & Rujiravanit, 2008) and titania (anatase) nanowires (Zhang & Qi, 2005).

According to the previous work, the ammonia gas-enhancing *in situ* co-precipitation method has been proven to be an effective method for incorporating of the magnetic nanoparticle into nanofibrous matrix of BC (Katepetch, & Rujiravanit, 2011). The morphology of as-prepared magnetic nanoparticle-incorporated BC sample were showed the homogeneously dispersed of magnetic nanoparticle throughout the matrix of BC. Moreover, the particle size of magnetic nanoparticle was still retained in the nanometer scaled-diameter even at 51.69 wt % incorporation of magnetic nanoparticle. Due to the advantages of the ammonia gas-enhancing *in situ* co-precipitation method, this preparation method was expected to also be an

effective preparation method for homogeneously incorporating of the Ag nanoparticle into the BC matrix. Moreover, the incorporating Ag nanoparticles were expected to completely coat on the surface of nanofibril BC to form the conduction pathway and finally, the as-prepared Ag nanoparticle incorporated-BC sample was exhibited the high electrical conductivity. In general, the synthetic route for Ag nanoparticle which dealed with ammonium hydroxide was the Tollens process as shown in schematic 1.

$$Ag(NH_3)_2^+(aq) + RCHO(aq) \longrightarrow Ag(s) + RCOOH(aq)$$

Schematic1 the synthetic route of Ag nanoparticle by using the Tollens process.

Firstly, the Ag^+ were formed the complex with ammonium hydroxide. The $Ag(NH_3)_2^+$ was reacted with aldehydes or reducing sugars (reducing agent) and then converted to Ag nanoparticle (Yin, Li, Zhong, Gates, Xia, & Venkateswaran, 2002). In order to use the ammonia gas-enhancing *in situ* co-precipitation method for preparing of the Ag nanoparticle incorporated-BC, the Tollen was developed by using the concept of *in situ* synthesis method; the precursor was firstly mixed or incorporated into an organic matrix then crystallization of such particles was performed inside an organic matrix. The $AgNO_3$ and glucose were firstly prepared as a precursor solution. Then, the BC pellicles were immersed into a precursor solution. Due to the unique porous structure of BC, the precursors, Ag^+ and glucose were readily penetrated through inside the BC pellicle. The precursor absorbed-BC pellicle was then treated with ammonia gas. During treating with ammonia gas, the Ag^+ was converted to Ag nanoparticle inside the nanofibrous matrix of BC.

In this study, the Ag nanoparticles were incorporated into the BC matrix by using ammonia gas-enhancing *in situ* synthesis method. In order to confirm the successfully formation of Ag nanoparticle inside the BC matrix, the as-prepared Ag nanoparticle-incorporated BC sample were characterized by various techniques such as UV-Vis spectroscopy, TEM, SEM and TGA. Finally, the electrical conductivity of the the as-prepared Ag nanoparticle-incorporated BC sample were determined by using the two-point probe conductivity measurement.

4.3 Experimental

4.3.1 Materials

Acetobacter xylinum (strain TISTR 975), an isolated strain in Thailand, was supplied from the Microbiological Resources Centre, Thailand Institute of Scientific and Technological Research (TISTR). Analytical grade anhydrous of D-glucose was obtained from Ajax Finechem. Bacteriological grade of yeast extract powder was purchased from HiMedia. Analytical grade of $AgNO_3$ was purchased from Ajax Finechem. Other chemical reagents used in this study were analytical grade and used without further purification.

4.3.2 Production of bacterial cellulose

The production process for BC was similar to our previous work (Katepetch, & Rujiravanit, 2011). Briefly, the pre-inocula for all the experiments were prepared by transferring a single colony of *A. xylinum* bacteria (strain TISTR 975) into 20 ml of a liquid culture medium, which was composed of 4 wt% g of D-glucose anhydrous, 1 wt% of yeast extract powder. After 24 h of cultivation at 30 °C, 2.5 ml of the cell suspension was introduced into a 200 ml-Erlenmeyer flask containing 25 ml of fresh liquid culture medium and then cultivated at 30 °C for 4 days. The obtained BC was purified by boiling in 1 % NaOH for 2 h. The boiling step was repeated twice. The purified BC was then treated with 1.5 % acetic acid for 30 min, and finally washed in a tap water until BC pellicles became neutral. The porous structure of BC was preserved by immersing into the distilled water and kept into a refrigerator at 4 °C prior to use.

4.3.3 The preparation of Ag particle incorporated-bacterial cellulose by ammonia gas-enhancing in situ synthesis method

$AgNO_3$ and glucose were used as a precursor. The precursor solution was prepared by dissolving the 0.01 mole of $AgNO_3$ and 0.1 mole of glucose in 1000 ml of distilled water. The mole ratio of Ag^+: glucose of the as-prepared precursor solution was corresponded to 1:10. After complete dissolution of AgNO3 and glucose, the BC pellicles were immersed in the precursor solution at room

temperature. In order to investigate the effect of mole ratio of Ag^+: glucose in the precursor solution on the average particle size of the as-prepared Ag nanoparticle, the concentration of $AgNO_3$ was fixed at 0.01 mole and the mole ratios of Ag^+: glucose were varied to be 1:10, 1:100 and 1:1000, respectively. After immersion of the BC pellicles in precursor solution for 1 h, the excesssive precursor solution on the surface of the BC pellicles was rinsed with distilled water. Then, the precursor absorbed-BC pellicles were kept inside 500 ml wide-neck round bottom flask (a reaction vessel) and pre-treated with nitrogen gas for 10 min in order to eliminate oxygen gas before further treating with ammonia gas. The volumetric flow rate of ammonia gas was controlled by a flow meter. When ammonia gas was purged into the reaction vessel, the color of precursor-absorbed BC pellicles was gradually changed. After 30 min of ammonia gas treatment, the as-prepared BC pellicle had yellowish brown color. The experimental set up for the ammonia gas-enhancing in situ synthesis method were showed in figure 4.1.The obtained BC pellicles were rinsed with a large amount of distilled water until neutral and then sonicated for 20 min in order to remove any loosely bound particles. Finally, the obtained samples were freeze dried and kept in a desicator. In order to investigate the effect of $AgNO_3$ concentration on the overall properties of the as-prepared Ag nanoparticle incorporated-BC sample, the mole ratios of Ag^+: glucose was fixed at 1:10 and the concentrations of $AgNO_3$ were varied to be 0.01, 0.025, 0.050, 0.075 and 0.100 M, respectively.

4.3.4 Characterization

The surface and cross-sectional morphology of the pristine BC were investigated by using the JEOL JSM-5200 scanning electron microscope (SEM). The effect of mole ratio of Ag^+: glucose in the precursor solution on the average particle size of the as-prepared Ag nanoparticle was investigated by UV-Vis spectroscopy (Shimazu) and TEM (JEOL JEM-2000EX). The TEM samples were prepared by embedding the freeze dried as-prepared Ag nanoparticle incorporated-BC samples in Spurr resin and performing ultrathin sectioning with a Reichert Ultracut E microtome equipped with a diamond knife. Histograms, average diameters and standard deviations were obtained by sampling 200 metal nanoparticles in TEM images of

100,000× magnification. The morphology of as-prepared Ag nanoparticle incorporated-BC samples were investigated by using the SEM (JEOL JSM-5200). The crystal structure of Ag nanoparticle inside the as-prepared Ag nanoparticle incorporated-BC sample was studied by the X-ray diffraction (XRD) (Rigaku). The as-prepared ZnO particle incorporated-BC samples were scanned from $2\theta = 20°$ to $2\theta = 80°$ at a scanning rate of 5° 2θ/min. The thermal stability of the as-prepared Ag nanoparticle incorporated-BC sample and percent incorporation of Ag particle inside the as-prepared Ag nanoparticle incorporated-BC sample were studied by using the thermogravimetric analysis (TGA, Perkin Elmer TGA7). The thermograms of the as-prepared ZnO particle incorporated-BC sample was in the temperature range from 50 to 750 °C with heating rate of 10 °C/min in a flow of air at 20 ml/min.

The electrical conductivity of the as-prepared Ag nanoparticle incorporated-BC samples were measured following the method of Ludeelerd, Niamlang, Kunaruksapong, & Sirivat (2010). The as-prepared Ag nanoparticle incorporated-BC samples were cut into a dish shape with 1 cm in diameter. The Keithley, Model 8009 probe was used for measuring electrical conductivity of the as-prepared Ag nanoparticle incorporated-BC sample. The constant voltage was supplied by Keithley, Model 6517A which connecting to the measured-probes and the measured-probes were in contact with a surface of the as-prepared Ag nanoparticle incorporated-BC sample. The output current while applying voltage was measured. The output current was only measured in the linear Ohmic regime of each sample. The applied voltage and the resultant current were converted to the electrical conductivity the as-prepared Ag nanoparticle incorporated-BC samples by following equation

$$\sigma = 1/\rho = 1/(R_s \times t) = I/(K \times V \times t)$$

where σ is the specific conductivity (S/cm), ρ the specific resistivity (Ω cm), R_s the resistivity of the as-prepared sample (Ω), I the resultant current (A), K the geometric correction factor, V the applied voltage (voltage drop, V), and t the thickness of the as-prepared sample (cm).

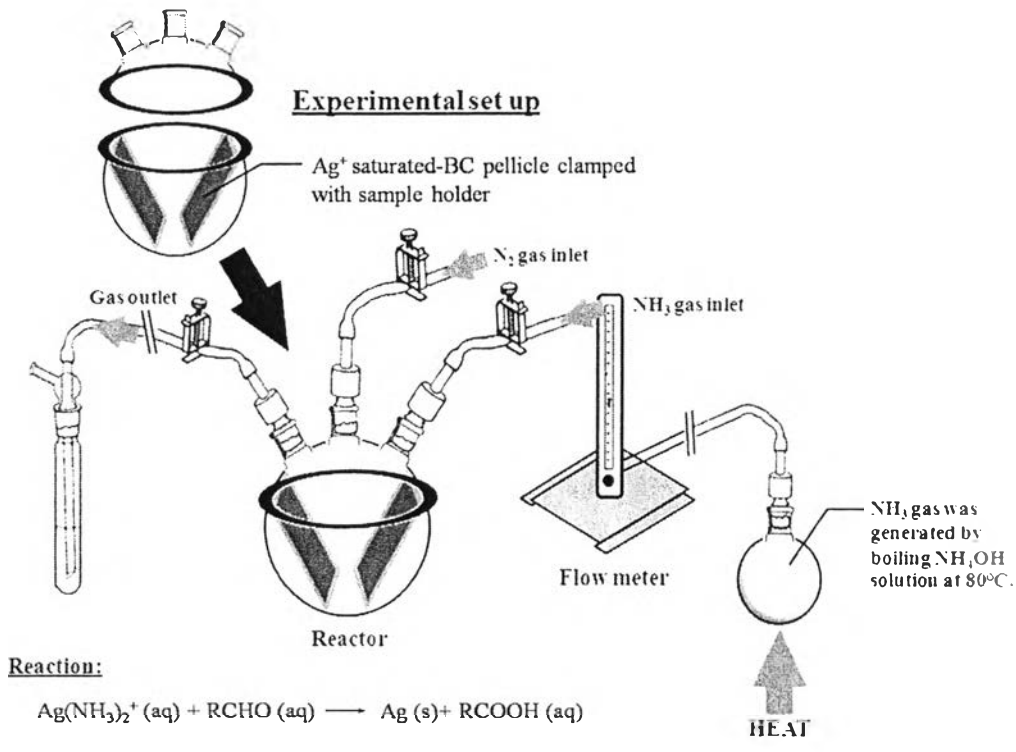

Figure 4.1 The experimental set up for preparing of the Ag nanoparticle incorporated-BC by using the ammonia gas enhanced-*in situ* synthesis method.

4.4 Results and Discussion

4.4.1 The preparation of Ag particle incorporated-BC by using the ammonia gas-enhancing in situ synthesis method

BC was purified cellulose which produced from *A. Xylinum* bacteria by using glucose as a carbon source. The BC was firstly generated at the interface between air and the culture surface. As long as the system is kept unshaken, BC pellicle was generated a layer by layer slides steadily downwards as it thickens (Iguchi, Yamanaka, & Budhiono, 2000). The surface and cross-sectional morphology of the pristine BC was showed in the figure 4.2. Regarding to the BC production process, the surface morphology of pristine BC showed the three dimensional non-woven network structure of nanofibrous cellulose with a fiber diameter of 55.00 ±10.54 nm. Whereas, the cross sectional morphology of BC showed the multilayer structure of BC membrane linked together with the cellulose nanofibrils as shown in

figure 4.2. The unique nanometer scale structure of BC was provided a large amount of surface hydroxyl groups. Therefore, the BC fibrous exhibited the super hydrophilic surface with represented in the form of hydrogel or never-dried state. The never-dried state of BC provided a good tunnel for Ag^+ penetration through inside BC which corresponding to the concept of *in situ* synthesis. Therefore, these unique physical structure of BC was firmly supported the ammonia gas-enhancing *in situ* synthesis method. The experimental set up for the ammonia gas-enhancing *in situ* synthesis method was showed in the figure 4.2. The BC pellicle was firstly immersed in the precursor solution which containing of $AgNO_3$ and glucose. During the immersion process of BC pellicle in the precursor solution, the precursors, Ag^+ and glucose were readily to penetrate though inside the BC matrix by passing through the microporous structure of BC pellicle. Moreover, the penetrated Ag^+ ions were trapped inside BC by the electrostatic interaction between the polar groups at the surface of BC nanofibrils such as hydroxyl or ether groups. Then, the Ag^+ absorbed-BC pellicles were treated with ammonia gas. While treating with ammonia gas, the Ag^+ ions were reacted with ammonium hydroxide to form silver ammonia complex, $Ag(NH_3)_2^+$. These complexes of Ag^+ were then reacted with the glucose and converted the silver ammonia complex to be the Ag nanoparticle (Yin, Li, Zhong, Gates, Xia, & Venkateswaran, 2002). The synthetic route for Ag nanoparticle by using the Tollen reagents as a precursor was showed in schematic 1. According to the unique structure of BC pellicle, the precursor was homogeneously penetrated through inside BC matrix which resulted in the homogeneously dispersion of Ag nanoparticles after treating with ammonia gas. After treating with ammonia gas, the color of the as-prepared BC pellicle was gradually changed from a yellow to a yellowish brown and to a brown with an increasing of the mole ratio of Ag^+: glucose from 1:10 to 1:100 and to 1:1000, respectively. The formation of the Ag nanoparticles inside the as-prepared Ag nanoparticle incorporated-BC sample was investigated by the UV-Vis spectroscopy. The figure 4.3 showed the UV-Vis absorption spectra of the as-prepared Ag particle incorporated-BC prepared from the Ag^+: glucose molar ratio of 1:10, 1:100 and 1:1000. These spectra showed the characteristic absorption spectra of the metallic silver nanoparticles inside the as-prepared Ag particle incorporated-BC due to the surface plasmon resonance (SPR) of

conducting electron (or free electron) on the surface of Ag nanoparticles (Kim & Kang, 2004). The UV-Vis absorption spectral of the as-prepared Ag-particle incorporated-BC sample which prepared from the mole ratio of Ag: glucose 1:1000, 1:100 and 1:10 were observed at 484, 529 and 556 nm, respectively. Moreover, the UV-Vis absorption spectral of the as-prepared Ag-particle incorporated-BC sample were tend to broaden with decreasing of the mole ratio of Ag^+: glucose from 1:1000 to 1:100 and to 1:10, respectively. The red shifted and broaden of the UV-Vis absorption spectral of the as-prepared Ag-particle incorporated-BC sample were represented to the larger particle size and the boarder size distribution of the incorporated-Ag particle. The effect of mole ratio of Ag^+: glucose in the precursor solution on the particle size of the incorporated-Ag particle was also confirmed by the TEM images. Figure 4.4 showed TEM images and histograms of the as-prepared Ag particle-incorporated BC samples prepared by ammonia gas-enhanced *in situ* synthesis with the mole ratio of Ag^+: glucose was 1:10 (a and d), 1:100 (b and e) and 1:1000 (c and f), respectively. As shown in Figure 4.4a and d, irregular shape of silver particles with large particle size and wide size distribution were obtained at the Ag^+: glucose molar ratio of 1:10. Their mean diameter (d) and standard deviation (σ) were 24.19 and 8.63 nm, respectively. When the Ag^+: glucose molar ratio was increased from 1:10 to 1:100 and to 1:1000, the Ag particles were more regular shape and also the particle size was decreased from 24.19 ±8.63 nm to 17.24 ±6.05 nm and to 13.67 ±3.03 nm, respectively. The larger particle size and the boarder size distribution of the incorporated-Ag nanoparticle with decreasing of the mole ratio of Ag: glucose might result from the excess amount of Ag^+ ions were aggregated to be a large particle. In order to achieve the excellent electrical conductivity, the particles need to be well connected to form the conduction pathway. The well connected of Ag particle could be control by the particle size of the as-synthesized Ag particle. Therefore, the well connected of Ag particle could also be control by the mole ratio of Ag^+: glucose in precursor solution.

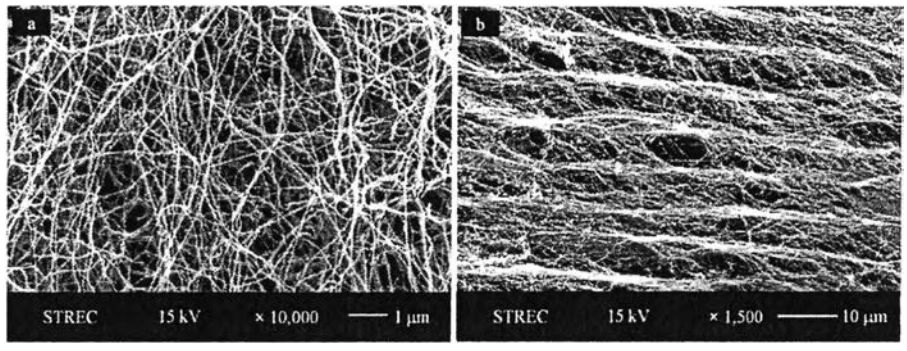

Figure 4.2 Surface and cross-sectional morphology of pristine BC at the magnification of 10,000× (a) and 1,500× (b), respectively.

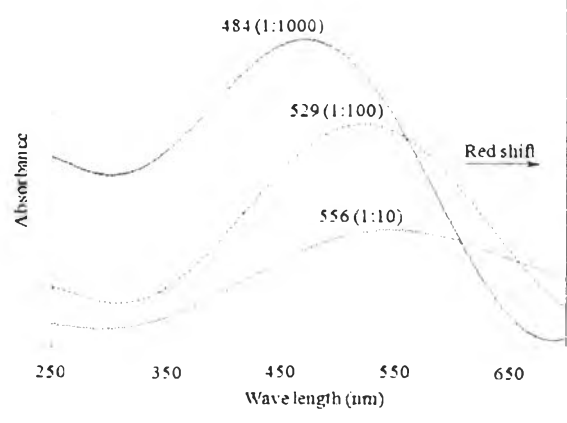

Figure 4.3 The UV-Vis absorption spectra of the as-prepared Ag particle incorporated-BC prepared from the Ag^{+}: glucose molar ratio of 1:10, 1:100 and 1:1000.

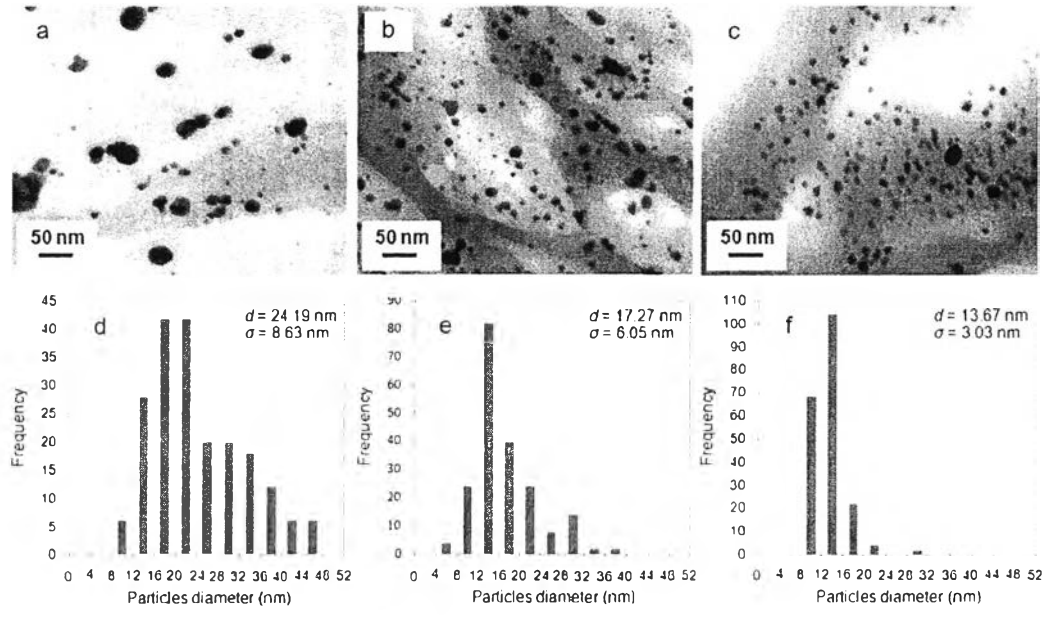

Figure 4.4 TEM images and histograms of the as-prepared Ag particle-incorporated BC samples prepared by ammonia gas-enhanced *in situ* synthesis with the mole ratio of Ag^+: glucose was 1:10 (a and d), 1:100 (b and e) and 1:1000 (c and f), respectively.

4.4.2 Morphology of the as-prepared Ag particle incorporated-BC prepared by ammonia gas-enhancing in situ synthesis method

The morphology of the as-prepared Ag particle incorporated-BC sample was investigated by SEM. Figure 4.5a showed the surface morphology of the pristine BC. The pristine BC exhibited the three-dimensional non woven network structure of nanofibrous cellulose with a fiber diameter of 55.00 ±10.54 nm. The morphology of the as-prepared Ag particle incorporated-BC samples, prepared by using ammonia gas enhanced *in situ* synthesis method with the concentration of $AgNO_3$ in precursor solution were varied to be 0.010 (Figure 4.5b), 0.025 (Figure 4.5c), 0.050 (Figure 4.5d), 0.075 (Figure 4.5e), 0.100 M (Figure 4.5f) and the mole ratio of Ag^+: glucose was fixed at 1:10, were exhibited the three-dimensional non woven network structure of nanofibrous cellulose which incorporated with Ag particle. The average particle size of the incorporated-Ag particle which were determined by using SEM images were corresponded to the average particle size of

the incorporated-Ag particle which were determined by using TEM images in that the particle size of incorporated-Ag particle were in the range of nanometer scale in diameter. The average particle size of the incorporated-Ag particle was slightly increased with increasing the concentration of $AgNO_3$ in the precursor solution. Anyways, the incorporated-Ag particle tended to aggregate and coated on the surface of nanofibrous cellulose. At the $AgNO_3$ concentration of 0.010 M (figure 4.5b), the discrete particles of the incorporated-Ag particles were observed at the surface of BC fibril. By increasing the concentration of $AgNO_3$ in the precursor solution from 0.010 to 0.025 and to 0.050 M, the amount of the incorporated-Ag particles was increased and tended to aggregate to be a bulk of Ag particle cover on the surface of BC fibril. These discrete bulks of Ag particle were also increased and tend to completely cover the BC fibril by increased the precursor solution from 0.050 to 0.075 and to 0.100 M, respectively. The amount of the incorporated-Ag particle was tend to reach a saturated point at the concentration of $AgNO_3$ in precursor solution was 0.075 M. The electrical conductivity of the as-prepared Ag particle incorporated-BC sample was directly related on the connectivity of the incorporated-Ag particles. By adjusting the concentration of $AgNO_3$ and the mole ratio of Ag^-: glucose in the precursor solution, the particle size and the connectivity of the incorporated-Ag particle could be control therefore the electrical conductivity of the as-prepared Ag particle incorporated-BC sample could also trailer made by the concentration of $AgNO_3$ and the mole ratio of Ag^+: glucose in the precursor solution.

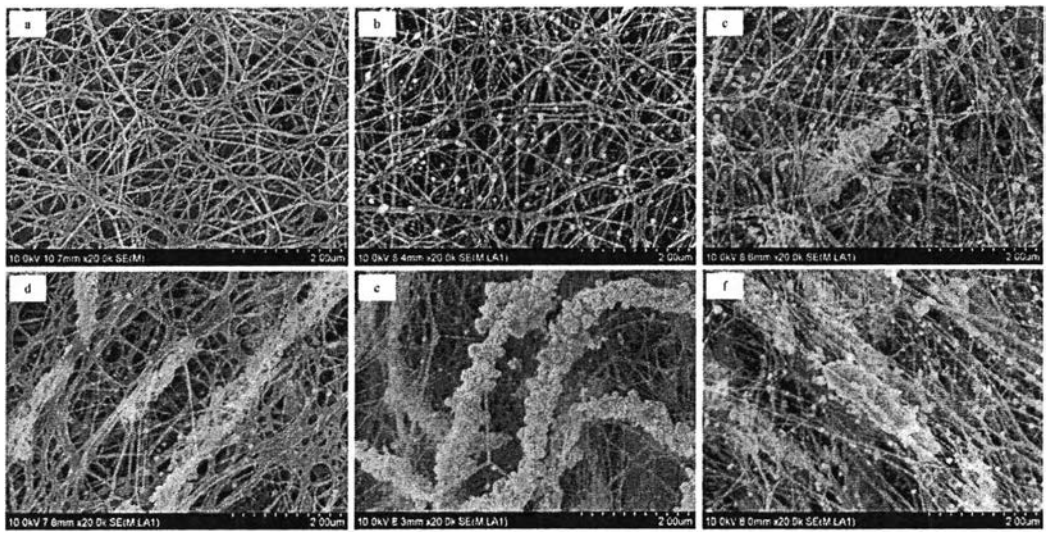

Figure 4.5 The surface morphology of the pristine BC (a) and the as-prepared Ag particle-incorporated BC samples prepared by ammonia gas-enhanced *in situ* synthesis, the concentration of $AgNO_3$ in the precursor solution were varied to be 0.010 (b), 0.025(c), 0.050(d), 0.075(e) and 0.100 M, respectively.

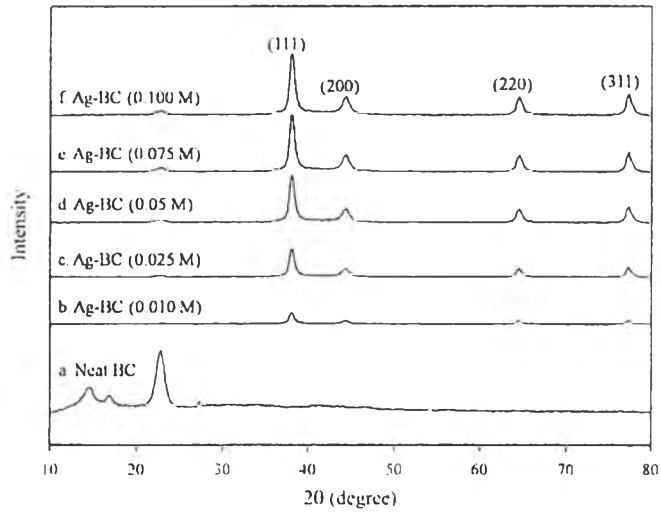

Figure 4.6 X-ray diffraction spectra of pristine BC (a) and the as-prepared Ag particle-incorporated BC sample prepared by ammonia gas-enhancing *in situ* synthesis method with using precursor solution of 0.010 (b), 0.025 (c), 0.050 (d), 0.075 (e) and 0.100 M (f), respectively; the mole ratio of Ag^+: glucose in the precursor solution was fixed at 1:10

4.4.3 *The crystal structure of Ag particle in the as-prepared Ag particle incorporated-BC sample*

The crystal structure of Ag particle in the as-prepared Ag particle incorporated-BC sample was investigated by the X-ray diffraction technique. Figure 4.6 showed the representative XRD spectrum of pristine BC (a) and the Ag particle incorporated-BC prepared by the ammonia gas-enhanced *in situ* synthesis method at the 0.010 (b), 0.025 (c), 0.050 (d), 0.075 (e) and 0.100 M (f) of $AgNO_3$ with the mole ratio of Ag^+: glucose was fixed at 1:10. The XRD pattern of pristine BC was exhibited the 2 characteristic peaks of BC at 2□ = 14.5° and 22.7°. These 2 characteristic peaks were corresponded to (110) and (220) planes, respectively which attributed to the typical profile of cellulose I allomorph (Retegi, Gabilondo, Peña, Zuluaga, Castro, Gañan, Caba, & Mondragon, 2010). This characteristic diffraction pattern was corresponded to the BC cultured in static culture (Yan, Chen, Wang, Wang, Wang, & Jiang, 2008). All the XRD patterns of the as-prepared Ag particle incorporated-BC sample (figure 4.6b-f) showed the similar characteristic diffraction patterns with the similar characteristic diffraction peaks at 2θ = 38.1°, 44.3 °, 64.4 ° and 78.0 °. These 4 characteristic diffraction peaks of Ag particle incorporated BC were corresponded to (111), (200), (220) and (311) planes, respectively. All these characteristic diffraction peaks indicated that the as-synthesized Ag particles were face centered cubic (fcc) structure (Jiang, Wang, Chen, Yu, & Wang, 2005; Zhang, Liu, Dai, Feng, Bao, & Mo, 2006). According the XRD pattern and SEM immages, there were clearly revealed that the Ag particles were successfully incorporated into the nanofibrous matrix of BC by using the ammonia gas-enhancing *in situ* synthesis method.

4.4.4 *Thermal gravimetric analysis (TGA) of the as-prepared Ag particle incorporated-BC sample*

The thermal stability of pristine BC and the as-prepared Ag particle incorporated-BC sample was studied by the TGA. The investigated temperature was ranged from 50°C to 750°C. All thermograms were recorded under the nitrogen atmosphere in order to prevent the oxidation reaction between as-prepared samples

and oxygen gas. Figure 4.7a showed the TGA thermograms of the pristine BC and the as-prepared Ag particle incorporated-BC sample prepared by ammonia gas-enhancing *in situ* synthesis method at various preparation conditions. The thermogram of pristine BC in the figure 4.7a showed the main weight loss between 275 °C to 375 °C as a result of the thermal decomposition of BC. These include depolymerization, further dehydration, degradation of the glucopyranosyl units and subsequent oxidation leaving behind charred residues (Roman & Winter, 2004). All thermograms of as-prepared Ag particle-incorporated BC sample were quite similar to the thermogram of pristine BC in term of the degradation temperature which the occurrence of main weight loss between 300 °C to 375 °C. The differences in onset thermal degradation temperature of BC between the pristine BC and the as-prepared Ag particle incorporated-BC sample might result from the incorporated-Ag particles. The incorporated-Ag particle were improved the thermal stability of the as-prepared Ag particle incorporated-BC sample therefore the onset degradation temperature of the as-prepared Ag particle incorporated-BC sample were shifted from 275 °C to 300 °C.

The percent incorporation of Ag particles in Ag particle incorporated-BC sample was also examined by using TGA (Ghule *et al.*, 2006). The total percent weight loss of pristine BC was 91.67 ±0.69 wt % and the residue from thermal decomposition of BC was 8.33 ±0.69 wt %. The residue from thermal decomposition of BC was attributed to vestigial carbon of BC whereas the total percent weight loss of the as-prepared Ag particle incorporated-BC sample prepared by ammonia gas-enhancing *in situ* synthesis method with 0.010, 0.025, 0.050, 0.075 and 0.100 M of $AgNO_3$ in the precursor solution were 81.87 ±0.47, 66.58 ±0.38, 50.17 ±0.30, 42.50 ±0.46 and 36.87 ±0.39 wt %, respectively. The difference in percent weight loss between pristine the BC and the as-prepared Ag particle incorporated-BC sample was attributed to be the percent incorporation of Ag particle in the as-prepared Ag particle incorporated-BC sample. The percent incorporation of Ag particle in the as-prepared Ag particle incorporated-BC sample were 9.80 ±0.53, 25.09 ±0.46, 41.50 ±0.42, 49.17 ±0.51 and 54.79 ±0.46 wt % at the concentration of $AgNO_3$ in the precursor solution to be 0.010, 0.025, 0.050, 0.075 and 0.100 M, respectively (as shown in Figure 4.7b). The percent incorporation of Ag particle in the as-prepared

Ag particle-incorporated BC sample was remarkably increased with increasing of the concentration of $AgNO_3$ in the precursor solution from 0.010 M to 0.025 M and to 0.050 M, respectively. However, when the concentrations of $AgNO_3$ in the precursor solutions were further increased from the 0.050 M to 0.075 M and to 0.100 M, the percent incorporation of Ag particle in the as-prepared Ag particle-incorporated BC sample were slightly increased and tended to reach equilibrium at a concentration of aqueous iron ion solution higher than 0.075 M. The percent incorporation of Ag particle in the as-prepared Ag particle incorporated-BC sample were corresponded to the SEM image in that the amount of Ag particle from SEM image were tend to saturated at the concentration of $AgNO_3$ in the precursor solution was 0.75 M.

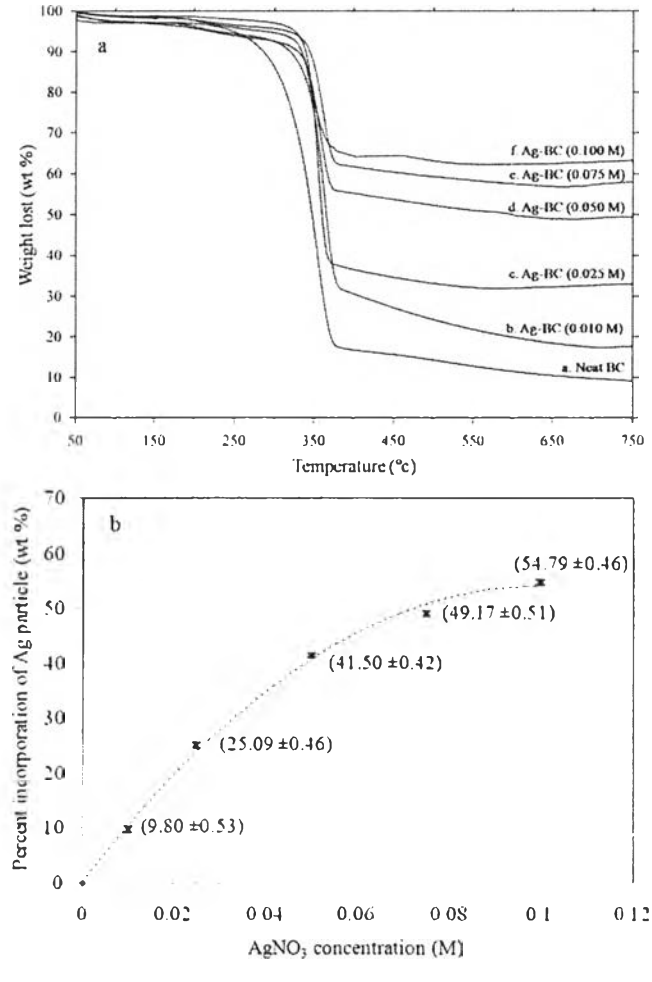

Figure 4.7 TGA thermograms of pristine BC (a) and compared to the Ag particle incorporated-BC which were prepared by ammonia gas-enhancing *in situ* synthesis method with 0.010 (b), 0.025 (c), 0.050 (d), 0.075 (e) and 0.100 M (f) of $AgNO_3$, respectively and the mole ratio of Ag^+: glucose was fixed at 1:10. Inset showed the percent incorporation of Ag particle in the as-prepared Ag particle incorporated-BC sample with increasing of the Ag^+ concentration in precursor solution. The percent incorporation of Ag particle is the difference in weight loss when compared to the pristine BC.

4.4.5 The electrical conductivity of the as-prepared Ag particle incorporated-BC sample

The electrical conductivity of pristine BC and the as-prepared Ag particle incorporated-BC sample was investigated by using the two point probe conductivity meter following the method of Ludeelerd, Niamlang, Kunaruksapong, & Sirivat (2010). The output current in the linear Ohmic regime was measured while applying voltage. The applied voltage and the resultant current were converted to the electrical conductivity the as-prepared Ag nanoparticle incorporated-BC samples by using the sample thickness and the geometric correction factor of the two point probe conductivity meter. Figure 4.8 showed the electrical conductivity of pristine BC and the as-prepared Ag particle-incorporated BC sample prepared by ammonia gas-enhancing *in situ* synthesis method with using precursor solution of 0.010, 0.025, 0.050, 0.075 and 0.100 M of $AgNO_3$, respectively; the mole ratio of Ag^+: glucose in the precursor solution was fixed at 1:10. The electrical conductivity of pristine BC was 6.34×10^{-4} S/cm where as the electrical conductivity of the as-prepared Ag particle-incorporated BC sample prepared by using 0.010 M of $AgNO_3$ was 2.60×10^{-4} $\pm5.31\times10^{-5}$ S/cm. When the concentration of $AgNO_3$ in the precursor solution was increased from 0.010 to 0.025 and to 0.050 M, the as the electrical conductivity of the as-prepared Ag particle-incorporated BC sample was increased from to 2.60×10^{-4} $\pm5.31\times10^{-5}$ to1,282.85 ±55.63 and to 1,686.38 ±153.28 S/cm, respectively. Moreover, the electrical conductivity of the as-prepared Ag particle-incorporated BC sample was still increased from 1,686.38 ±153.28 to 1981.08±187.19 S/cm with increasing of the $AgNO_3$ concentration from 0.050 to 0.075 M. Finally, the electrical

conductivity of the as-prepared Ag particle-incorporated BC sample was reached to the equilibrium at the $AgNO_3$ concentration of 0.100 M with the electrical conductivity of 2,188.32 ±120.82 S/cm. The increasing in electrical conductivity of the as-prepared Ag particle-incorporated BC sample with increasing the $AgNO_3$ concentration in the precursor solution was resulted from the increasing in the amount of the incorporated-Ag particle with increasing the $AgNO_3$ concentration. According to the figure 4.8, the electrical conductivity of the as-prepared Ag particle incorporated-BC sample was dramatically increased from 2.60×10^{-4} $\pm5.31\times10^{-5}$ to1,282.85 ±55.63 S/cm with increasing of the $AgNO_3$ concentration in the precursor solution from 0.010 to 0.025 M. Whereas, the electrical conductivity of the as-prepared Ag particle incorporated-BC sample was slightly increased and reached an equilibrium with further increasing of the $AgNO_3$ concentration in the precursor solution. The dramatically increased in the electrical conductivity of the as-prepared Ag particle incorporated-BC sample was called "percolation threshold" (Sandler, Kirk, Kinloch, Shaffer, & Windle, 2003). These were resulted from the well connected of the incorporated-Ag particles to form the continuous conduction pathway therefore the electrical conductivity of the as-prepared Ag particle incorporated-BC sample was dramatically increased from 2.60×10^{-4} $\pm5.31\times10^{-5}$ to1,282.85 ±55.63 S/cm. Due to the dramatically increased in the electrical conductivity of the as-prepared Ag particle incorporated-BC sample, the electrical properties of the Ag particle incorporated-BC could classified as conductive material (electrical conductivity > 10^3). Another well-known preparation method for the Ag nanoparticle-impregnated BC which developed by our group was the *in situ*-synthesis of Ag nanoparticle into BC matrix by using sodium borohydride ($NaHBO_4$) as a reducing agent (Maneerung, Tokura, & Rujiravanit, 2008). The Ag nanoparticle-impregnated BC was prepared by immersing of BC pellicle into 0.025 M of $AgNO_3$ at room temperature for 1 h. The Ag^+ absorbed-BC pellicle was then immersed in the 0.25 M of $NaHBO_4$ solution at room temperature for 30 min. Finally, the obtained Ag nanoparticle impregnated-BC samples were dried by using the freeze drying process. The obtained Ag nanoparticle impregnated-BC samples prepared by the *in situ*-synthesis of Ag nanoparticle into BC matrix by using $NaHBO_4$ as a reducing agent were exhibited the electrical conductivity of 582.40 ±300.56 S/cm. Regarding

to the electrical conductivity, the obtained Ag nanoparticle impregnated-BC samples prepared by the *in situ*-synthesis of Ag nanoparticle into BC matrix by using $NaHBO_4$ as a reducing agent were classified as semiconductive material. In comparison with the *in situ*-synthesis of Ag nanoparticle into BC matrix by using $NaHBO_4$ as a reducing agent, the ammonia gas-enhanced *in situ* synthesis method was exhibited the much higher in the electrical conductivity of the as-prepared sample. The much higher in the electrical conductivity of the sample might result from the advantages of the preparation method. The ammonia gas-enhanced *in situ* synthesis method had been proof to be an effective preparation method in that the incorporated-metal particles were homogeneously distributed throughout the matrix of BC (Katepetch, & Rujiravanit, 2011). Whereas, the *in situ*-synthesis of Ag nanoparticle into BC matrix by using $NaHBO_4$ as a reducing agent were mainly generated the Ag nanoparticles at the surface of BC pellicle. The obtained Ag nanoparticle impregnated-BC pellicles prepared by the *in situ*-synthesis of Ag nanoparticle into BC matrix by using $NaHBO_4$ as a reducing agent showed the darker skin at the surface resulted from the predominant generation of Ag nanoparticles at the surface of the BC pellicles (Maneerung, Tokura, & Rujiravanit, 2008). Moreover, the $NaHBO_4$ was acted as an effective reducing agent for Ag particle resulted in the smaller size of the as-prepared Ag particle (Maneerung, Tokura, & Rujiravanit, 2008). The smaller size and the bad distribution of the as-prepared Ag particle might result in the discontinuous of the conduction pathways leading to the low electrical conductivity of the as-prepared samples.

Moreover, the maximum electrical conductivity of the as-prepared Ag particle incorporated-BC sample prepared by the ammonia gas-enhancing *in situ* synthesis method was 2188.32 ±120.82 S/cm whereas the electrical conductivity of the copper plate was 1749.68 ±35.47 S/cm. The much higher in the electrical conductivity of as-prepared Ag particle incorporated-BC sample might resulted from the homogeneously distribution of the incorporated-Ag particles leading to the continuous conduction pathway.

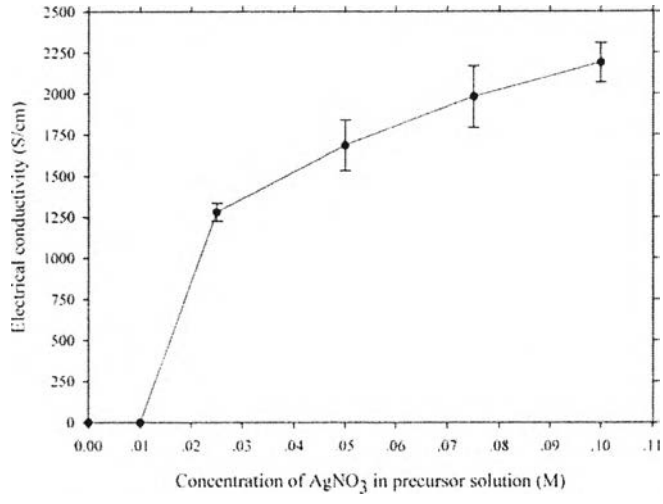

Figure 4.8 The electrical conductivity of pristine BC and the as-prepared Ag particle-incorporated BC sample prepared by ammonia gas-enhancing *in situ* synthesis method with using precursor solution of 0.010, 0.025, 0.050, 0.075 and 0.100 M, respectively; the mole ratio of Ag^{+}: glucose in the precursor solution was fixed at 1:10.

For a comparison, the magnetic particle-incorporated bacterial cellulose pellicles were also prepared by the step-wise dipping process according to the method of Sourty, Ryan, and Marcessault (1998) and digital images of the obtained products are shown in Figures 3.2a, 3.2b and 3.2c. Briefly, bacterial cellulose pellicles were firstly dipped in an aqueous iron salt solution contained $FeCl_3$ and $FeSO_4$ with the mole ratio of the Fe^{3+} to Fe^{2+} ions of 2 to 1, followed by dipping in a fresh solution of 30% ammonia solution. The total concentrations of aqueous iron ion were varied to be 0.01 M (Figure 3.2a), 0.05 M (Figure 3.2b), and 0.1 M (Figure 3.2c). The obtained bacterial cellulose pellicles showed the darker skin at the surface which resulted from the predominant precipitation of magnetic particles at the surface of the bacterial cellulose pellicles. On the other hand, the magnetic particle-incorporated bacterial cellulose pellicles prepared by ammonia gas-enhanced *in situ* co-precipitation method had homogeneous dark color of magnetic particles across the cross-sectional area of the sample as shown in Figures 3.2d, 3.2e and 3.2f. The colors of magnetic particles in the bacterial cellulose

pellicles changed from yellow to dark brown and black when the total concentrations of aqueous iron ion were increased from 0.01 M (Figure 3.2d) to 0.05 M (Figure 3.2e) and 0.1 M (Figure 3.2f). The homogeneous dark color across the cross-sectional area of the sample implied the homogeneous dispersion of the precipitated magnetite particles across the cross-section area of bacterial cellulose pellicles.

The use of ammonia gas instead of a concentrated liquid basic solution could improve the homogeneous dispersion of the magnetic particles across the cross-sectional area of the as-synthesized bacterial cellulose pellicles since the ammonia gas is easier to penetrate through the bacterial cellulose pellicles than using concentrated liquid basic solutions. Moreover, ammonia gas could slightly increase pH of the sample and prevent the predominant precipitation of magnetic particles at the surface of bacterial cellulose pellicles.

4.5 Conclusions

In this study, the Ag nanoparticles were successfully in situ synthesis into the nanofibrous matrix of BC by using the ammonia gas-enhancing *in situ* synthesis method. The synthesis route was modified the Tollen process by using the concept of *in situ* synthesis method. Firstly, the Tollen precursor, Ag^+ and glucose were incorporated into the nanofibrous matrix of BC by using simple immersion of BC pellicle into the precursor solution. The precursor solution was a solution mixture of $AgNO_3$ and glucose. Due to the unique morphology of BC pellicle, the Ag^+ and glucose could easily penetrate through inside the porous structure of BC matrix. Moreover, the penetrated-Ag^+ ions were trapped inside the porous matrix of BC by interaction with the polar groups such as hydroxyl or ether groups at the surface of BC nanofibrial. Then, the Ag^+-absorbed BC pellicles were treated with ammonia gas in the closed system of reaction vessel. During the purging of ammonia gas, the Ag^+ ions inside the BC matrix were formed complex with NH_4OH. These just formed-complexes could further react with the glucose to form Ag particle inside the nanofibrous matrix of BC pellicle. The formation of the Ag nanoparticle in the matrix of BC was investigated by UV-Vis spectroscopy and TEM. The UV-Vis absorption peaks were corresponded with the TEM images in that the particle size of

the as-prepared Ag particle were decreased with increased with increasing the mole ratio Ag^+:glucose. The particle size of the Ag particle inside the as-prepared Ag particle incorporated-BC were decreased from 24.19 ±8.63 nm to 17.24 ±6.05 nm and to 13.67 ±3.03 with increasing the mole ratio of Ag^+:glucose from 1:10 to 1:100 and to 1:1000, respectively. The effect of the $AgNO_3$ concentration in the precursor solution on the overall properties of the as-prepared Ag particle incorporated-BC sample were investigated by various techniques such as XRD, SEM, TGA and two point probe conductivity meter. The XRD patterns of the as-prepared Ag particle incorporated-BC sample were showed all four characteristic peaks of the incorporated-Ag particles which indicated that the Ag particle in the as-prepared Ag particle incorporated-BC sample were in the form of face-center cubic (FCC) structure. The SEM images of the as-prepared Ag particle incorporated-BC sample were clearly revealed the formation of Ag nanoparticles on the surface of nanofibrous BC. By increasing the $AgNO_3$ concentration in the precursor solution, the amount Ag nanoparticles were increased and tended to aggregate cover the nanofibril of BC. The result from SEM images were also corresponded to the percent incorporation of the Ag particle in the as-prepared Ag particle incorporated-BC sample in that the percent incorporation of the Ag particle in the as-prepared Ag particle incorporated-BC sample was increased with increasing the $AgNO_3$concentration of the precursor solution. The percent incorporation of the Ag particle in the as-prepared Ag particle incorporated-BC sample were increased from 9.80 ±0.53 to reach an equilibrium at 54.79 ± 0.46 wt % with the concentration of $AgNO_3$ in the precursor solution was increased from 0.010 to 0.100 M, respectively. Finally, the electrical properties of the as-prepared Ag particle-incorporated-BC sample were studied by using two point probe conductivity meter. The electrical conductivity of the as-prepared Ag particle incorporated-BC sample were dramatically increased from 2.60×10^{-4} ±5.31×10^{-5} to1,282.85 ±55.63 S/cm with increasing of the $AgNO_3$ concentration in the precursor solution from 0.010 to 0.025 M. Then, the electrical conductivity of the as-prepared Ag particle incorporated-BC sample were further increased with increasing of the $AgNO_3$ concentration in the precursor solution and reached to the equilibrium at 0.100 M of $AgNO_3$ with the electrical conductivity of 2,188.32 ±120.82 S/cm. Due to the advantages of the

ammonia gas-enhancing *in situ* synthesis method preparation method, the incorporated-Ag particles were homogeneously dispersed in the matrix of BC. These homogeneously dispersion of Ag particles in the matrix of BC were from the conduction pathway therefore the as-prepared Ag particle incorporated-BC sample was exhibited the excellent electrical conductivity. Anyways, in comparison with the *in situ* synthesis of Ag nanoparticle into BC matrix by using $NaHBO_4$ as a reducing agent, the ammonia gas-enhancing *in situ* synthesis method still exhibited the many advantages in that the as-prepared Ag particle incorporated-BC sample prepared from the ammonia gas-enhancing *in situ* synthesis method showed the electrical conductivity in the range of conductive material whereas the as-prepared Ag particle incorporated-BC sample prepared from the *in situ* synthesis of Ag nanoparticle into BC matrix by using $NaHBO_4$ as a reducing agent showed the electrical conductivity in the range of semiconductive material. All of these evidences were clearly revealed that the ammonia gas-enhancing in situ synthesis method was one of the effective methods for preparing of the Ag particle incorporated-BC. Moreover, this new proposed-preparation method was surprisingly simple, cost-effective and environmental friendly, which may provide a facile approach toward the manufacturing of metal oxide nanocomposites, antimicrobial materials, low-temperature catalysts and other useful materials. By using this preparation method, the electrically responsive properties also could be achieved into the other materials such as electro-spun nanofiber mat and other porous materials.

4.6 Acknowledgements

This work is greatly supported in cash and in kind by the Chulalongkorn University Dutsadi Phiphat Scholarship, the Rachadapisek Somphot Endowment Fund, The Petroleum and Petrochemical College, Chulalongkorn University, The Conductive and Electroactive Polymers Research Unit, Center of Excellence on Petrochemical and Materials Technology and Kansai University, Japan, are greatly acknowledged.

4.7 References

Czaja, W. K., Romanovicz, D., & Brown, R. M., (2004). Structural investigations of microbial cellulose produced in stationary and agitated culture. *Cellulose, 11*, 403–411.

Czaja, W. K., Young, D. J., Kawecki, M., & Brown, R. M. (2007). The future prospects of microbial cellulose in biomedical applications. *Biomacromolecules, 8*, 1–12.

Dubey, V., Saxena, C., Singh, L., Ramana, K. V., & Chauhan R. S. (2002). Pervaporation of binary water–ethanol mixtures through bacterial cellulose membrane. *Separation and Purification Technology, 27*, 163–171.

Fugetsua, B., Sanob, E., Sunadac, M., Sambongic, Y., Shibuyac, T., Wangd, X., & Hirakid, T. (2008). Electrical conductivity and electromagnetic interference shielding efficiency of carbon nanotube/cellulose composite paper. *carbon, 46*, 1253-1269.

Ghule, K., Ghule, A. V., Chen B., & Ling, Y. (2006). Preparation and characterization of ZnO nanoparticles coated paper and its antibacterial activity study. *Green Chemistry, 8*, 1034–1041.

Grzegorczyn, S., & Ezak, A. (2007). Kinetics of concentration boundary layers buildup in the system consisted of microbial cellulose biomembrane and electrolyte solutions. *Journal of Membrane Science, 304*, 148–155.

Haes, A. J. & Van Duyne, R. P. (2003). Nanosensors Enable Portable Detectors for Environmental and Medical Applications. *Laser Focus World, 39*, 153–156.

Hiamtup, P., Sirivat, A., & Jamieson, A. M. (2008). Electromechanical response of a soft and flexible actuator based on polyaniline particles embedded in a cross-linked poly(dimethyl siloxane) network. Materials *Science and Engineering C, 28*, 1044–1051.

Hu, W., Chen, S., Li, X., Shi, S., Shen, W., Zhang, X., & Wang, H. (2009). In situ synthesis of silver chloride nanoparticles into bacterial cellulose membranes. *Materials Science and Engineering C, 29*, 1216–1219.

Hu, W., Chen, S., Zhou, B., & Wang, H. (2010). Facile synthesis of ZnO nanoparticles based on bacterial cellulose. *Materials Science and Engineering B, 170*, 88–92.

Iguchi, M., Yamanaka, S., & Budhiono, A. (2000). Bacterial cellulose–A masterpiece of nature's arts. *Journal of Materials Science, 35(2)*, 261–270.

Jiang, G. H., Wang, L., Chen, T., Yu, H. J., & Wang, J. J. (2005). Preparation and characterization of dendritic silver nanoparticles. *Journal of Materials Science, 40*, 1681–1683.

Kamel, S. (2007). Nanotechnology and its applications in lignocellulosic composites, a mini review. *eXPRESS Polymer Letters, 1*, 546–575.

Katepetch, C., & Rujiravanit, R. (2011). Synthesis of magnetic nanoparticle into bacterial cellulose matrix by ammonia gas-enhancing *in situ* co-precipitation method. *Carbohydrate Polymers, 86*, 162–170.

Kim, Y. H., & Kang, Y. S. (2004). Synthesis and characterization of Ag nanoparticles, Ag–TiO2 nanoparticles and Ag–TiO2–chitosan complex and their application to antibiosis and deodorization. *Materials Research Society, 820*, 161–166.

Li, X., Chen, S., Hu, W., Shi, S., Shen, W., Zhang, X. & Wang H. (2009). In situ synthesis of CdS nanoparticles on bacterial cellulose nanofibers. *Carbohydrate Polymers, 76*, 509–512.

Ludeelerd, P., Niamlang, S., Kunaruksapong, R., & Sirivat, A. (2010). Effect of elastomer matrix type on electromechanical response of conductive polypyrrole/elastomer blends. *Journal of Physics and Chemistry of Solids, 71*, 1243–1250.

Lu, Y., & Chou, K. (2008). A simple and effective route for the synthesis of nano-silver colloidal dispersions. *Journal of the Chinese Institute of Chemical Engineers, 39*, 673–678.

Magdassi, S., Bassa, A., Vinetsky, Y. & Kamyshny, A. (2003). Silver Nanoparticles as Pigments for Water-based Ink-Jet Inks. *Chemistry of materials, 15*, 2208–2217.

Maneerung, T., Tokura, S., & Rujiravanit, R. (2008). Impregnation of silver nanoparticles into bacterial cellulose for antimicrobial wound dressing. *Carbohydrate Polymers, 72*, 43–51.

Niamlang, S., & Sirivat, A. (2009). Electrically controlled release of salicylic acid from poly(p-phenylene vinylene)/polyacrylamide hydrogels. *International Journal of Pharmaceutics, 371*, 126–133.

Nie, S. & Emory, S. R. (1997). Probing Single Molecules and Single Nanoparticles by Surface-enhanced Raman Scattering. *Science, 275*, 1102–1106.

Pradhan, N., Pal, A., & Pal, T. (2002) Silver Nanoparticle Catalyzed Reduction of Aromatic Nitro Compounds. *Colloids and Surfaces A: Physicochemical and Engineering Aspects, 196 (2)*, 247–257.

Retegi, A., Gabilondo, N., Peña, C., Zuluaga, R., Castro, C., Gañan, P., Caba, K., & Mondragon, I. (2010). Bacterial cellulose films with controlled microstructure–mechanical property relationships. *Cellulose, 17*, 661–669.

Rezaee, A., Solimani, S., & Forozandemogadam, M. (2005). Role ofplasmid in production of Acetobacter xylinum biofilms. *American Journal of Biochemistry and Biotechnology, 1*, 121–125.

Roman, M., & Winter, W. T. (2004) Effect of sulfate groups from sulfuric acid hydrolysis on the thermal degradation behavior of bacterial cellulose. *Biomacromolecules, 5*, 1671–1677.

Sandler, J.K.W., Kirk, J. E., Kinloch, I. A., Shaffer, M. S. P., & Windle, A. H. (2003). Ultra-low electrical percolation threshold in carbon-nanotube-epoxy composites. *Polymer, 44*, 5893–5899.

Thuwachaowsoan, K., Chotpattananont, D., Sirivat, A., Rujiravanit, R., & Schwank J. W. (2007) Electrical conductivity responses and interactions of poly(3-thiopheneacetic acid)/zeolites L, mordenite, beta and H2. *Materials Science and Engineering B, 140*, 23–30.

Wan, Y., Hong, L., Jia, S., Huang, Y., Zhu, Y., Wang, Y., & Jiang, H. (2006). Synthesis and characterization of hydroxyapatite-bacterial cellulose nanocomposites. *Composites Science and Technology, 66*, 1825–1832.

Yin, Y., Li, Z., Zhong, Z., Gates, B., Xia, Y., & Venkateswaran, S. (2002). Synthesis and characterization of stable aqueous dispersions of silver nanoparticles through the Tollens process. *Journal of Material Chemistry, 12*, 522–527.

Ye, L., Lai, Z., Liu, J., & Tholen, A. (1999). Effect of Ag Particle Size on Electrical Conductivity of Isotropically Conductive Adhesives. *IEEE TRANSACTIONS on Electronics Packaging Manufacturing, 22 (4)*, 299–302.

Yan, Z., Chen, S., Wang, H., Wang, B., Wang, C., & Jiang, J. (2008). Cellulose synthesized by Acetobacter xylinum in the presence of multi-walled carbon nanotubes. *Carbohydrate Research, 343*, 73–80.

Zhang, D., & Qi, L. (2005). Synthesis of mesoporous titania networks consisting of anatase nanowires by templating of bacterial cellulose membranes. *Chemical Communications, 21*, 2735–2737.

Zhang, J., Liu, K., Dai, Z., Feng, Y., Bao, J., & Mo, X. (2006). Formation of novel assembled silver nanostructures from polyglycol solution. *Materials Chemistry and Physics, 100*, 106–112.

Zhang, R., Moon, K., Lin, W., Agar, J. C. & Wong, C. (2011). A simple, low-cost approach to prepare flexible highly conductive polymer composites by *in situ* reduction of silver carboxylate for flexible electronic applications. *Composites Science and Technology, 71*, 528–534.

Zuluaga, R., Putaux, J. L., Cruz, J., Ve´lez, J., Mondragon, I., & Gañan, P. (2009). Cellulose microfibrils from banana rachis: effect of alkaline treatments on structural and morphological features. *Carbohydrate Polymers, 76*, 51–59.